Cellular Signalling 93 (2022) 110270

Contents lists available at ScienceDirect

Cellular Signalling

journal homepage: www.elsevier.com/locate/cellsig

CKAP4 contributes to the progression of vascular calcification (VC) in chronic kidney disease (CKD) by modulating YAP phosphorylation and MMP2 expression

Yuping Shi [a,1], Xiucai Jin [b,1], Man Yang [a], Jieshuang Jia [a], Hui Yao [a], Weijie Yuan [a], Kui Wang [c,*], Shu Rong [a,*]

[a] Department of Nephrology, Shanghai General Hospital, Shanghai Jiaotong University School of Medicine, China
[b] Department of Ultrasound, Changhai Hospital, Naval Medical University (Second Military Medical University), China
[c] Department of Hepatic Surgery (II), Eastern Hepatobiliary Surgery Hospital, Navy Medical University (Second Military Medical University), China

ARTICLE INFO

Keywords:
Chronic kidney disease (CKD)
Vascular calcification (VC)
VSMCs
CKAP4
YAP
MMP2

ABSTRACT

Chronic kidney disease (CKD) is an growing public health concern associated with high mortality rates. The occurrences of vascular calcification (VC) increase concordantly with the progression of CKD.With CKD, hyperphosphatemia promotes intermediate VC, a process that is further facilitated by vascular smooth muscle cells (VSMCs) initiating osteogenic transdifferentiation. The purpose of this study was to determine the involvement of CKAP4 in VC progression. Clinical investigations demonstrate that elevated blood CKAP4 and matrix metallopeptidase 2 (MMP2) levels are related with CKD in individuals. As an *in vitro* model, mouse VSMCs were extracted and treated with high levels of phosphates (2.5 mmol/L Pi). We also created an *in vivo* mice model of CKD induced by 5/6 nephrophrectomies and a high-protein diet (High Pi diet). The expression of CKAP4 and MMP2 in both *in vitro* and *in vivo* models was significantly higher in VSMCs and calcified aorta in both models. Additionally, *in vitro* tests indicated that CKAP4 modulates YAP phosphorylation. Simultaneous silencing of CKAP4 and calcium content assay revealed a significant reduction in the VSMCs and calcium content of the aorta. Alizarin red staining and calcium content assay reveled that silencing of CKAP4 reduced the VSMCs and aortic calcification, accompanied with reduced expression of YAP and MMP2. Overall, our study demonstrates for the first time that CKAP4 contributes to VC in CKD by modulating YAP phosphorylation and MMP2 expression.

1. Introduction

Chronic kidney disease (CKD) has lately been identified as a serious public health burden, with a global prevalence of 13% [1,2]. CKD is classified into five stages based on renal glomerular filtration rates (GFR), with less than 60 mL/min per 1.73 m^2 being mild stage III CKD. Lower GFR levels result in more severe CKD development, including severe stage IV and end-stage V CKD [3]. Vascular calcification (VC) is a highly regulated process that resembles bone development in its mechanism [4], and is defined by the transition of contractile vascular smooth muscle cells (VSMCs) to an osteogenic phenotype [5]. Recent research suggests that arterial calcification contributes to increased cardiovascular mortality and morbidity, particularly in patients with CKD [6,7]. Typically, vascular function is typically defined by three distinct functions: endothelium secretion, smooth muscle contraction, and vascular structural integrity. Anomalies in one or more of these functions begin in the early stages of CKD alongside cardiovascular complications and progressively deteriorate as the illness advances to the end stage [8]. CKD-related CVD (cardiovascular disease) increases the risk of type 2 diabetes in patients, and even mild to severe CKD increases the risk of atherosclerosis by 87% [9,10]. Some patients have a combined severity of renal bone disease and VC, particularly during hemodialysis, which complicates therapy options [11].

In response to damage or stress, VSMCs in blood vessels play a critical role in redesigning and mending wounded portions [12,13]. It was previously established that calcification in VSMCs begins with the release of hydroxyapatite-containing vesicles [14]. This is followed by the active transition of VSMCs into an osteogenic or chondrogenic

* Corresponding authors.
E-mail addresses: wangkuiykl@smmu.edu.cn (K. Wang), shu.rong@shgh.cn (S. Rong).
[1] Yuping Shi and Xiucai Jin contributed equally to this work.

https://doi.org/10.1016/j.cellsig.2022.110270
Received 3 August 2021; Received in revised form 24 January 2022; Accepted 26 January 2022
Available online 30 January 2022

lineage, which promotes the release of vesicular structures. Additionally, the osteogenesis of these cells induces mineralization and the release of many substances such as alkaline phosphatase (ALP) and bone morphogenic factor, allowing VSMCs to totally transform into osteogenic cells [15]. VSMCs, on the other hand, passively recruit minerals from extracellular fluid and precipitate them in the vascular walls, increasing mineralization [16]. VC is frequently accompanied with elevated calcium and phosphate levels, which contributes to the vicious cycle of mineralization [15,17]. Studies have indicated that excessively high-phosphate levels can contribute considerably to CKD and are being used to construct models to better understand disease progression [18,19]. Surprisingly, VSMCs appear to be unable to adapt in a high phosphate environment, undergoing rapid differentiation and apoptosis [17]. Despite the fact that it is evident that VC is a substantial contributor to morbidity and mortality in individuals with CKD, the molecular basis for VC development is still unknown.

Cytoskeleton-associated protein 4 (CKAP4, also known as P63, CLIMP-63, and ERGIC-63) is an endoplasmic reticulum protein that is present on the surface of cell membranes, including VSMCs [20], and acts as a receptor for Dickkopf1 (DKK1) [21]. DKK1 has been implicated in the pathophysiology of VC [22]. In addition to DKK1, CKAP4 as a receptor can bind to APF (Antiproliferative factor), and CKAP4 binding to APF can inhibit Matrix Metalloproteinase-2 (MMP-2) production in T24 bladder cancer cells [23]. Additionally, MMP-2 overexpression causes arterial vascular calcification in patients with CKD [24]. Besides, DKK1 has been demonstrated to influence the activity of smooth muscle cells via the YAP-TEAD pathway [25]. In the research of gastric cancer, inhibiting YAP expression inhibited cell proliferation and metastasis by downregulating MMP-2 expression, demonstrating that YAP had a positive regulatory effect on MMP-2 [26]. Therefore, we hypothesize that CKAP4 can regulate YAP and MMP in some way, thereby regulating VC during chronic kidney disease. To create new diagnostic and therapeutic options, we sought to elucidate the molecular mechanisms underlying disease progression in this work. Initially, we discovered that CKD patients had elevated serum levels of a CKAP4, which suggests that CKAP4 may contribute to the VC process during CKD. Using an *in vitro* VSMC and an *in vivo* 5/6 Nx mice model fed a high-phosphate (Pi) media/diet, the current work sought to determine the precise mechanism by which CKAP4 acts in this process.

2. Materials and methods

2.1. Patients

Between May 2018 and July 2020, 142 CKD patients were recruited from the Nephrology Department at Shanghai General Hospital, with 57 men and 85 women ranging in age from 40 to 76. The control group in this study consisted of 32 healthy patients with normal renal function. All patients were given signed consent papers. Furthermore, studies were carried out in line with the Helsinki Declaration. The patient diagnoses are summarized in Table 1.

Table 1
Clinical characteristics of healthy volunteers and patients with CKD.

	Healthy controls	CKD stage III-IV	CKD stage V	*P*-value
No. of cases	32	47	95	
Age(years)	46.5 ± 6.5	57.9 ± 8.9	66.2 ± 10.1	0.06
Male gender(%)	56.2%	57.5%	61.1%	0.76
Hypertension(%)	–	55.2%	57.6%	
Diabetes mellitus(%)	–	58.5%	67.2%	
Serum creatinine(mg/dL)	0.63 ± 0.3	1.82 ± 0.25	5.95 ± 0.37	<00001
eGFR(mL/min/1.73m^2)	88.92 ± 4.4	29.85 ± 3.6	13.8 ± 2.4	<00001

Data are shown as mean ± S.E.M.

2.2. VSMCs culture and treatments

The VSMCs were cultured as previously described [16]. Briefly, umbilical veins were isolated and the endothelium was removed, the remaining part of the veins were split into smaller parts and cultured on lumen-coated plates. The explants were cultured in M199 medium containing 10% fetal calf serum (FCS) and 2 ng/ml basic FGF and were maintained at 37 °C in the presence of 5% CO_2. Complete medium replacement with fresh M199 medium was performed post 72 h. Within 2 weeks, cells emerged from the explant and confluency was achieved by 4 weeks. Smooth muscle identity was confirmed through α-smooth muscle actin (α-SMA) staining and the "hill and valley" growth patterning of the cells. Once the cells had undergone 5–8 passages, experiments were performed.

2.3. Animal model

All procedures were performed with respect to the guidelines and was approved by the Institutional Animal Care and Ethics committee at Shanghai Jiaotong university. A total of 80 male C57BL/6 J mice (8–10 weeks) were purchased form Jackson Laboratory, Sacramento, CA. The 5/6NX model was developed in male C57BL/6 J mice, and the detailed operation method was based on a previously published paper [27]. Further, the mice were kept at 12 h light and 12 h dark cycle in a (19–21 °C) temperature-maintained facility with standard rodent diet and access to drinking water. The 5/6 Nx model (CKD group, $n = 60$) was developed on C57BL/6 J mice by decapsulating the left kidney through flank incision and resection of the upper and lower poles. Post 1 week, another surgery, specifically by incision in the right flank the right kidney was removed entirely. Sham group ($n = 20$) mice underwent similar surgical procedure except for the removal of right kidney. Post 1-week recovery, mice from both sham and CKD group were randomly split equally into two groups with either a normal (0.5%) phosphate (normal Pi) diet or high (1.5%) phosphate diet (high Pi) for 12 weeks. To further explore the role of CKAP4 in CKD *in vivo*, two weeks after CKD model developed, 24 mice from the CKD group that was fed High Pi were chosen randomly. They were then split into two groups with 12 mice each. One group was given 100 μl of CKAP4 siRNA lentivirus at a dose of 10^7 vector geneome per mice via tail vein injection, and the other group got the same amount of scramble siRNA. Further, after 12 weeks, using computerized tail-cuff system, blood pressure of the mice was measured. Urine was also assessed using ELISA kits (Assay Designs, Ann Arbor, MI) for creatinine and protein levels. Mice were successfully sacrificed with 50 mg/kg pentobarbital and renal tissues were removed for further processing. These tissues were either quickly fixed and processed using Mason's staining or flash frozen using liquid nitrogen and stored at −80 °C for further analysis.

2.4. Calcium deposition

To assess the deposited calcium, cells were initially decalcified for 24 h using HCl (0.6 mol/L). Calcium concentration was measured from the supernatant using absorption spectroscopy. The BCA assay kit was used to quantify the protein recovered from the cells (Pierce, Rockford, IL) and were used to achieve normalization of the samples.

2.5. 3-(4,5-Dimethylthiazol-2-yl)-2,5-diphenyltetrazolium bromide (MTT) assay

To determine cell viability, VSMCs were seeded at a density of 4×10^3 cells/well on a 96 well plate. The cells were allowed to grow for 48 h and were incubated with MTT solution (Sigma Chemical Co., USA) at a concentration of 5 mg/ml at 37 °C. After 4 h of incubation, the MTT solution was removed and 100 μl DMSO was added. To allow complete

solubility of the intracellular purple crystals, cells were incubated in an orbital shaker with DMSO for 5 mins. Further at 570 nm, absorbance was measured using a microplate reader (Thermo, Rockford, IL). Further, cell viability percentage was calculated using the formula "OD of treatment group/OD of control group * 100".

2.6. Alizarin red staining

Calcification was determined using Alizarin red staining as previously described [28,29]. Briefly, cells seeded onto 6 well plate were fixed using 70% ethanol and stained with Alizarin red. Further, the accumulated stain was dissolved using ethylpyridium chloride and thus obtained supernatant was measured at 550 nm using a microplate reader.

2.7. Measurement of alkaline phosphatase (ALP) activity

Cells cultured on a 24 well plate were detached after reaching confluency and sonicated in the presence of 600 μl distilled water. Using a modified Lowry method, ALP activity was measured. Briefly, assay mixtures containing 0.1 M 2-amino-2-methyl-1-propanol, 8 mM p-nitrophenyl phosphate disodium, and 1 mM $MgCl_2$, were added onto the cell homogenates. Post 4 mins incubation at 37 °C, NaOH was used to inhibit the reaction. Further at 405 nm, absorbance was read using a microplate reader. Measurements *p*-nitrophenol was used to prepare the standard curve. Further, normalization of the values was achieved using protein concentrations which were measured from the sonicated samples using BCA method [30].

2.8. Apoptosis assay

Apoptotic cell death was assessed by staining the cells with Annexin-V FITC and PI- staining. Based on the manufacturer's protocols, both attached and free-floating cells were collected and stained with Annexin V-FITC antibody and PI. Further, these cells were quantified using flow cytometry [31].

2.9. Cell line and viral transduction

Overexpression of CKAP4 was performed using a lentivirus designed cDNA obtained from OriGene (Rockville, MD). 293A cells were used for production of CKAP4 containing lentivirus. To attain efficient transduction, a multiplicity of infection (MOI) of 100 was used.

2.10. Small interfering RNA (siRNA) transfection

NC-siRNA, CKAP4-siRNA and YAP-siRNA were synthesized chemically at Suzhou GenePharma Co. Ltd. (Suzhou, China). Mouse CKAP4 gene was constructed into pcDNA3.1 + HA vector by Life Technologies (Invitrogen, California, USA), and the empty vector served as the negative control. The cells were cultured to attain 70–80% confluency, after which cells were transfected either with, NC-siRNA or CKAP4-siRNA using Lipofectamine 2000 (Invitrogen, California, USA) based on the manufacturer's instructions.

2.11. Immunocytochemical staining

Firstly, cells were washed twice with PBS for 10 mins. Subsequently, they were fixed with 4% paraformaldehyde for 10 mins and permeabilized using 0.5% Triton-X in 0.1 M Tris-buffered saline (TBS; pH 7.6). Further, the cells were quickly washed with PBS. The cells were blocked 3% goat serum in TBS. Then, the cells were incubated with YAP (ab52771, Abcam) and MMP-2 (ab97779, Abcam) primary antibody diluted in TBS with normal goat serum (10%) for 1 h. Subsequently, the cells were incubated with the Alexa Red conjugated anti-mouse IgG (Molecular Probes) secondary antibody in TBS for 1 h. Nuclear staining was performed using Hoechst 33258. Subsequent imaging of the cells was performed using Laser Scanning confocal fluorescence microscope (Olympus FV1000S).

2.12. Immunohistochemical analysis

Paraffin embedded tissue sections (4 μm) were used to perform immunohistochemical analysis. The sections were mounted onto SUPERFROST slides and incubated at 37 °C overnight. De-waxing in xylene and ethanol was followed by antigen-retrieval by boiling in microwave oven three times for 5 mins (pH 6.0, 0.94 ml Antigen Unmasking Solution (Vector Laboratories, Burlingame, CA, USA)/100 ml distilled water). Further, the slides were immersed in 3% hydrogen peroxide solution for 20 mins. Blocking was performed with 10% goat serum in PBS for 30 mins. Slides were incubated with primary antibodies against CKAP4 (ab84712, Abcam) overnight at 4 °C which was subsequently followed by incubation with secondary antibody conjugated with hydrogen peroxidase for 30 mins. Visualization was achieved with the aid of 3-Amino-9-Ethylcarbazole (AEC) substrate chromogen (ADI-950-200-0003, WAKO) and utilized based on the manufacturer's instructions. The sections were stained with hematoxylin and dehydrated through the treatment with gradient ethanol. Finally, the sections were mounted and visualized.

2.13. Western blot analysis

Cells were cultured in 6 well dishes for 48 h and the protein was extracted RIPA buffer containing 0.1% SDS. The extracted protein was quantified using BCA assay kit. 20 μg of protein denatured using Lamelli buffer were loaded and migrated using a 10–15% SDS-PAGE gel, transferred onto a nitrocellulose membrane. Blocking of the membranes were performed using 5% skim milk in PBST (PBS with 0.1% Tween-20) for 1 h. Further, the membranes were incubated with the same blocking buffer containing either of the primary antibodies; anti-CKAP4 (Abcam, 1:1000), anti-YAP (Abcam, 1:1000), anti-α-SMA (Abcam, 1:1000), anti-RUNX2 (Abcam, 1:1000), anti-Pit1 (Abcam, 1:1000), anti-MMP2 (Abcam, 1:1500), anti-Caspase-3 (Abcam, 1:1000), anti-Bax (Abcam, 1:1000), anti-MST1 (Abcam, 1:500), anti-p-MST1 (Abcam, 1:1000), anti-LATS1 (Abcam, 1:1000), anti-p-LATS1 (Abcam, 1:1500), anti-GAPDH (Abcam, 1:2000), anti-MMP2 (Abcam, 1:1000), and anti-SM22α (Bioss, 1:1000). The blots were incubated at 4 °C overnight. Further, the blots were washed with PBST thrice and 5 mins each. The membranes were subsequently incubated with secondary antibody conjugated with horse-radish peroxidase for 1 h at RT. The membranes were visualized using chemiluminescent reagent in accordance with the manufacturer's instructions. The quantitative results of western blot analysis were determined in Image J software (U. S. National Institutes of Health, Bethesda, MD, USA).

2.14. QRT-PCR

The total RNA in samples were isolated using TRIZOL reagent (Invitrogen). After quantification, cDNA was synthesized using the First-strand cDNA synthesis kit (Invitrogen). A light cycler (Roche) and FastStart DNA Master Plus SYBR green I kit (Roche) was used to perform the quantitative PCR. Further, the expression was normalized with the values obtained from GAPDH. PCR conditions used in this study is a as follows 95 °C for 15 s, 57 °C for 30 s, and 72 °C for 1 min. The primers used in the study are summarized below: CKAP4-F: TCCCGTCAGAGGGATGAGC, CKAP4-R: GCTGGGAGTTTCTCAGGAGG; MMP2-F: ACCTGAACACTTTCTATGGCTG, MMP2-R: CTTCCGCATGGTCTCGATG; YAP-F: TTGCGTCTGATCTCGTGGAG, YAP-R: GGAAGCTGTCTCATGCCTCA; α-SMA-F: TCCACCGCAAATGCTTCTAAGT, α-SMA-R: ATGAGTCAGAGCTTTGGATAGGC; SM22α-F: TGGTGAGCCAAGCAGACTTC, SM22α-R: AAGGCTTGGTCGTTTGTGGA; Pit1-F: CAATTCCGCCTCTGCACCTA, Pit1-R: TTCACATGTGTGCTGGCTTC;

Runx2-F: CCGCCTCAGTGATTTAGGGC, Runx2-R: GGGTCTGTAATCTGACTCTGTC; MSX-F: GGAGCACCGTGGATACAGG; MSX-R: TAGAAGCTGGGATGTGGTGAA; GAPDH-F: AGGTCGGTGTGAACGGATTTG, GAPDH-R: TGTAGACCATGTAGTTGAGGTCA.

2.15. Statistical analysis

Data presented in this study are representative of three independent experiments. The results are expressed as mean ± S.E.M. The significance of the values was assessed using one-way analysis of variance (ANOVA) followed by Student's *t*-test. All the statistical analysis in this study was carried out using SPSS 16.0 software. $P < 0.05$ was considered statistically significant.

2.16. Ethics statement

The present study was approved by the local investigational review board and written informed consent was obtained from all participants.

3. Results

3.1. High phosphates treated VSMCs based CKD in vitro model

Initially, we looked into the levels of CKAP4 and MMP2 in the patients with CKD. When comparing individuals with stage V CKD, who are regarded to have end stage renal illness, to normal people, we discovered that they had the highest levels of both CKAP4 and MMP2 when compared to normal patients. Additionally, CKAP4 and MMP2 levels were considerably elevated in patients with stage III-IV chronic kidney disease, indicating that they may play a role in the disease (Fig. 1A, B). To further understand the roles of CKAP4 in CKD, we initially developed an *in vitro* VSMCs model using umbilical veins as described in the methods section (see methods, VSMCs culture and treatments). Further, to induce calcification, the cells were treated with high phosphates (HP, 2.5 mmol/L Pi). Consequently, with increasing time (days) in culture, we could observe increased calcification through alizarin red staining in the HP group when compared to both normal Pi (NP, 1.5 mmol/L Pi) and osmotic control (OC, NP + 2.5 mmol/L D-mannitol) treatment groups (Fig. 1C, D, at day 7, $P < 0.01$). Alternatively, we also checked the ALP activity, which is an important indicator of CKD progression. HP treatment was shown to significantly increase ALP levels (Fig. 1E, $P < 0.01$). These evidences supported our hypothesis that cells treated with HP concentrations might serve as appropriate *in vitro* models for CKD. To further investigate the impact of CKD progression on the expression profiles of VSMCs markers, the VSMCs were treated with differentiation medium for 2 weeks to direct them either towards smooth muscle cell or osteogenic lineage.

In vivo, the phenotype transition of VSMCs is linked to VC. To verify the success of cell models used to simulate the progression of CKD *in vivo*, the expression of VSMC markers such as α-SMA and SM22α was studied as before [32]. Alternatively, we observed an increased expression of pituitary-specific positive transcription factor (PIT-1, bone mineralization factor, increased runt-related transcription factor 2 (Runx2, osteoblast differentiation factor), and increased msh homeobox 2 (MSX2, bone development marker). The data shown above further confirmed that our cell model accurately replicates the development of CKD by reducing smooth muscle differentiation and increasing osteogenesis (Fig. 1F, G). Using the MTT assay, we found that the HP-treated group had lower cell viability (Fig. 1H, $P < 0.01$). It was also evident from our Annexin-V flow cytometric analysis that HP treatment caused a severe 40% increase in apoptosis (Fig. 1I, J, $P < 0.001$). This was further affirmed through the increased cleaved caspase-3 and Bax expression in the HP treatment group (Fig. 1 K, L, $P < 0.01$).

3.2. Knockdown of CKAP4 reduces vascular calcification

To further understand the molecular role of CKAP4 in CKD, we silenced CKAP4 in VSMCs and treated them with HP using siRNA technology. Initially, we affirmed the successful silencing of CKAP4 by observing lower mRNA and protein levels in the si-CKAP4 group (Fig. 2A, B). Evidently, silencing also resulted in a reduction in calcification (Fig. 2C) and ALP activity (Fig. 2D, $P < 0.01$). This was supported by the fact that silencing of CKAP4 increased the levels of α-SMA, SM22α levels while decreasing PIT1, Runx2, MSX2 levels (Fig. 2E). This clearly indicated that a deficiency of CKAP4 inhibits osteogenesis and promotes smooth muscle formation. Additionally, we also observed increased cell viability (Fig. 2F) and apoptosis (Fig. 2G, H; $P < 0.001$) in the absence of CKAP4. The decreased apoptosis was also confirmed through decreased cleaved caspase-3 and Bax levels (Fig. 2I, J $P < 0.01$). Hence, the results indicate that CKAP4 could potentially play a vital role in the progression of CKD by regulating the differentiation of VSMCs toward the osteogenic lineage rather than the smooth muscle lineage.

3.3. CKAP4 is associated with nuclear translocation and phosphorylation of YAP

We further wanted to elucidate the molecular consequences of CKAP4, and were interested in a MMP2 regulator, Yes-associated protein (YAP). We identified that the absence of CKAP4 results in the translocation of YAP, which is normally localized in the nucleus. Immunofluorescence labeling revealed a 50% reduction in YAP nuclear localization following CKAP4 silencing (Fig. 3A,B). Hence, it could be possible that in the absence of CKAP4 there was an increased p-YAP-ser 127 protein which is considered the cytoplasmic version of YAP protein. Antibody identifying the nuclear and full version of the YAP showed decreased levels in the si-CKAP4 cells. Further, as YAP is a core component of the HIPPO pathway, we wanted to check the influence of CKAP4 on other HIPPO components such as large tumor suppressor 1/2 (LATS1/2) and mammalian sterile 20-like kinase 1/2 (MST1/2) and its phosphorylated versions. Evidentially, in the absence of LATS1/2 and MST1/2 were slightly decreased, when compared to the control group. However, the phosphorylated versions of both of these proteins where higher than the control group (Fig. 3C). This indeed mimicked the consequences observed in the YAP protein, indicating CKAP4 potentially affects CKD progression through the regulation of the HIPPO pathway.

As previous studies have indicated YAP as an upstream regulator of MMP2 [33], and in our study, we observed a high expression of MMP2 in the CKD patients, we sought to detect changes in MMP2 expression in response to YAP suppression. Using immunofluorescence staining, we identified and confirmed that absence of YAP decreased MMP2 levels significantly (Fig. 3D). Additionally, western blotting examination of the protein verified this (Fig. 3E). Interestingly, silencing of YAP also caused a severe decrease in calcification, as observed through alizarin red staining (Fig. 3F).

3.4. CKAP4 promotes VSMCs calcification via YAP/MMP-2 pathway

Furthermore, we intended to investigate the special role of CKAP4 in the calcification of VSMC. We studied the expression profile of smooth muscle and osteogenic markers in VSMCs with either si-CKAP4, si-CKAP4 + OV-MMP2 (silencing CKAP4 and overexpression of MMP2), OV-CKAP4 (overexpression of CKAP4), or OV-CKAP4 + si-MMP2 (overexpression of CKAP4 and silencing of MMP2). Initially, we compared the activity of ALP in each group (Fig. 3A). The results indicated that the decrease in ALP activity produced by CKAP4 interference could be compensated for by overexpression of MMP2, and that the rise in ALP activity caused by CKAP4 overexpression could be mitigated by MMP2 interference. We subsequently performed qRT-PCR and western blotting analysis for all the markers (Fig. 4A-H). When we overexpressed CKAP4; YAP, PIT1, Runx2, Msx2 were upregulated whereas α-SMA,

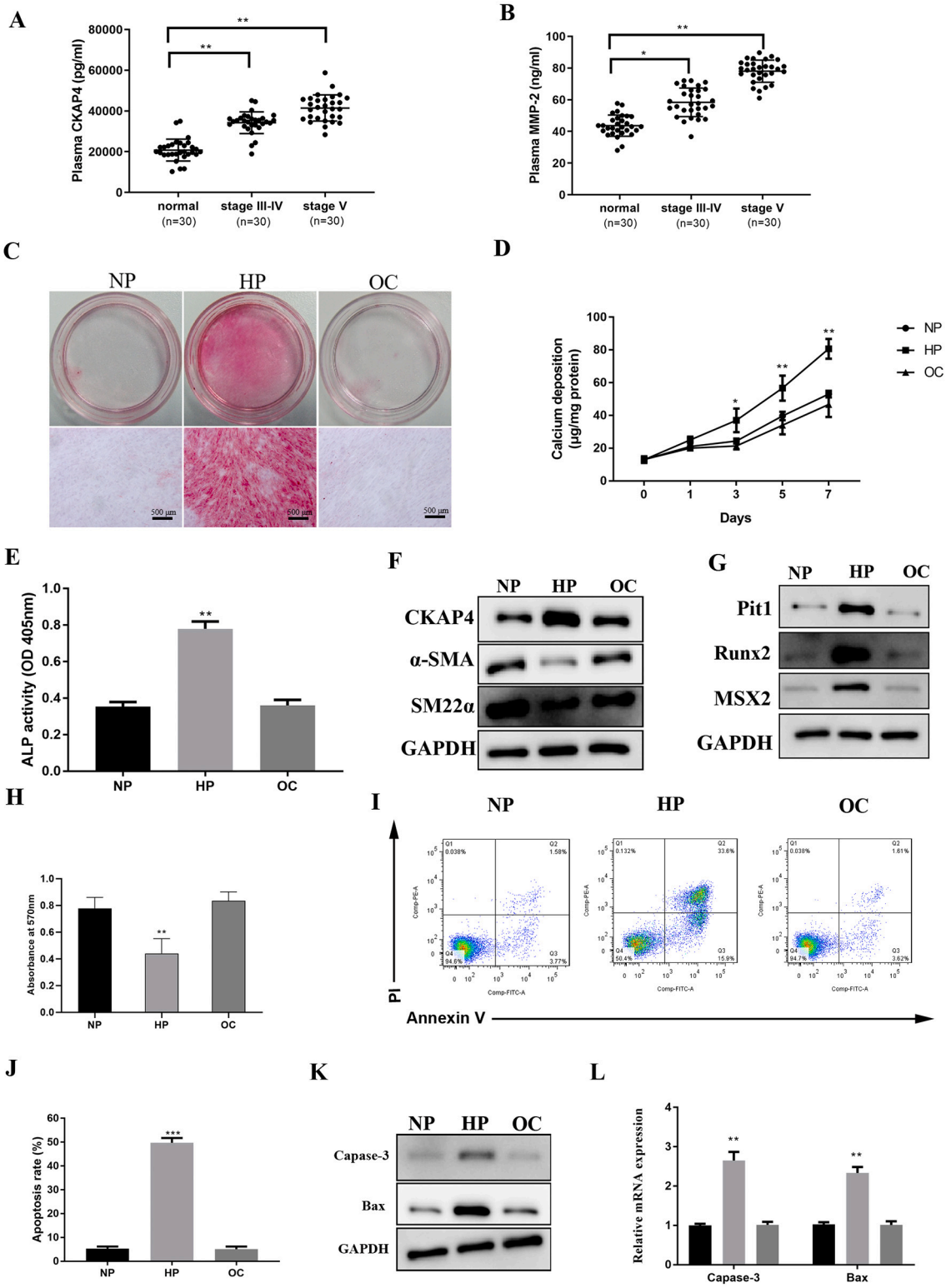

Fig. 1. Treatment with high phosphates induces VSMCs calcification. CKAP4 (A) and MMP2 (B) expression in the serum of patients with CKD detected by the ELISA kit. $^{*}P < 0.05$, $^{**}P < 0.01$. (C) Alizarin red staining was performed on VSMCs incubated under different conditions for 14 days with a media replacement every 3 days, $n = 3$. (D) Calcium content and (E) ALP activity was expressed as the mean ± S.E.M of at least three simultaneous replicates. (F,G) Expression of CKAP4, smooth cell and osteogenesis markers were determined through western blotting in VSMCs exposed to differentiation medium for 2 weeks, $n = 3$. (H) Cell viability was detected using MTT assay, $n = 3$. (I,J) Analysis of apoptosis rates were done using flow cytometry and quantification. Data are expressed as the mean ± S.E.M (n = 3). (K,L) Western-blot analysis of apoptosis related proteins (cleaved caspase-3 and Bax), $n = 3$. NP: Normal Pi (1.5 mmol/L Pi), HP: High Pi (2.5 mmol/L Pi), OC: Osmotic control (NP + 2.5 mmol/L D-mannitol). $^{**}P < 0.01$ compared to the NP treatment group.

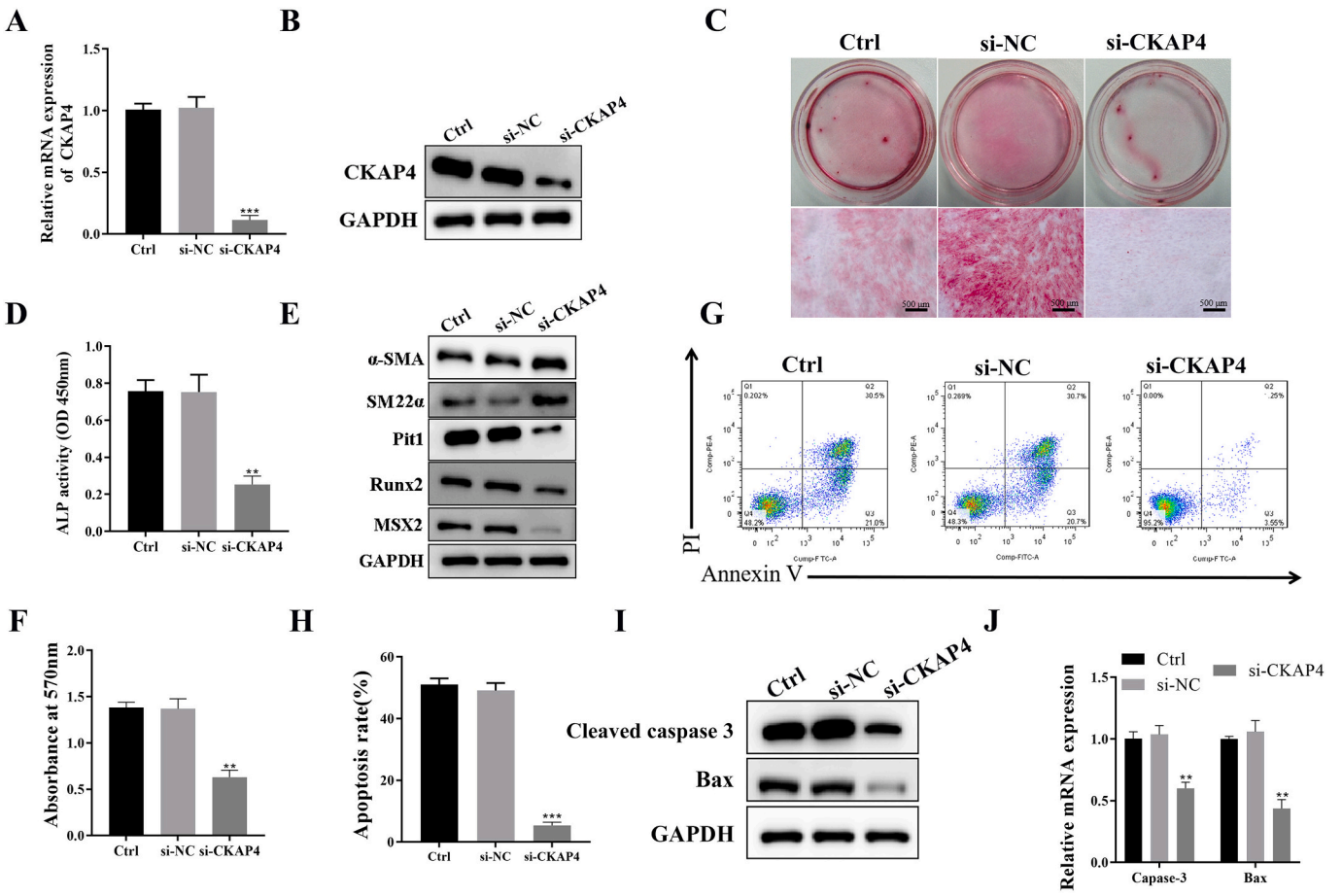

Fig. 2. Knockdown of CKAP4 reduces vascular calcification. VSMCs were treated with negative control, siRNA, or CKAP4 siRNA (si-CKAP4) for 24 h, respectively. The mRNA (A) and protein (B) expression of CKAP4 in VSMCS detected by RT-PCR and western blot analysis, respectively, $n = 3$. (C) Alizarin red staining was performed on VSMCs incubated under different conditions for 14 days with changing media every 3 days, $n = 3$. (D) ALP activity was expressed as the mean ± S.E.M, $n = 3$. (E) Expression of smooth cell and osteogenesis markers were determined by western blotting in VSMCs exposed to differentiation medium for 2 weeks, $n = 3$. (F) Cell viability was detected using MTT assay, n = 3. (G-H) Analysis of apoptosis rates by flow cytometry and quantification. Data are expressed as the mean ± S.E.M (n = 3). (I-J) Western blotting analysis of apoptosis related proteins (cleaved caspase-3 and Bax), $n = 3$. $^{**}P < 0.01$, $^{***}P < 0.001$ compared to the si-NC group.

SM22α were downregulated when compared with the silenced CKAP4. When comparing si-CKAP4 + OV-MMP2 to si-CKAP4 groups or OV-CKAP4 + si-MMP2 to si-CKAP4 groups revealed that MMP2 counteracted the facilitatory effects of CKAP4 on YAP, PIT1, Runx2, and Msx2 as well as the inhibitory effects on -SMA and SMA-like 22 (SM22) proteins. These evidences demonstrated that CKAP4 is sufficient to stimulate osteogenesis and calcification in VSMCs, and it regulated CKD progression through YAP/MMP2 pathway.

3.5. *High phosphate diet promotes CKAP4 expression and induces aortic calcification in a high CKD model*

To further validate our observations, we developed an *in vivo* 5/6 Nx mice model (CKD model), with high phosphate (Pi) diet. By using qRT-PCR and western blotting, we observed that the CKAP4 and MMP2 levels were significantly greater in the CKD model mice than those in the sham-operated group (Fig. 5A-C). Besides, high Pi diet in the CKD model group seems to further exacerbate the disease by a higher increase in CKAP4 and MMP2 levels when compared to normal Pi group in the CKD moedl group (Fig. 5A-C). These observations were confirmed using immunostaining of vascular tissue, which showed a severe CKAP4 increase in high Pi + CKD group, when compared with all the other groups (Fig. 5D).

To further validate the *in vivo* model, we checked the calcification in the aorta using alizarin red staining. Evidently, the degree of aortic calcification was substantially greater in the CKD model than in the Sham group mice, and the high Pi diet exacerbated the aortic calcification in the CKD group (Fig. 5E). Subsequently, we also confirmed the above-mentioned observations by quantifying the deposited calcium through absorption spectroscopic methods (Fig. 5F). Further, we observed in high Pi diet-CKD group, osteogenic markers (PIT1, Runx2, and Msx2) were highly upregulated. However, smooth muscle markers (α-SMA and SM22α) were highly downregulated (Fig. 5G). ALP activity was significantly higher in the both normal and high Pi-CKD group, when compared with sham group (Fig. 5H). However, ALP activity was most significantly increased in the high Pi-CKD group. Similarly, apoptotic rate was most severe in the high Pi-CKD group (Fig. 5I,J). This was subsequently confirmed with cleaved caspase-3 and Bax levels being most high in high Pi-CKD group (Fig. 5 K-M). Even though, 5/6 Nx CKD model could be the chief contributor for the CKD in these mice models, it was evident that its combination with high Pi diet leads to a severe CKD model.

3.6. *CKAP4 inhibition attenuates vascular calcification in CKD mice*

We additionally established another mice model, wherein CKD mice were administered with either scramble or si-CKAP4 lentivirus via tail vein injection and kept on high Pi diet for 12 weeks. Subsequently, the mice were sacrificed and tissues were assessed for calcification. It was clear that silencing of CKAP4 decreased calcification as observed

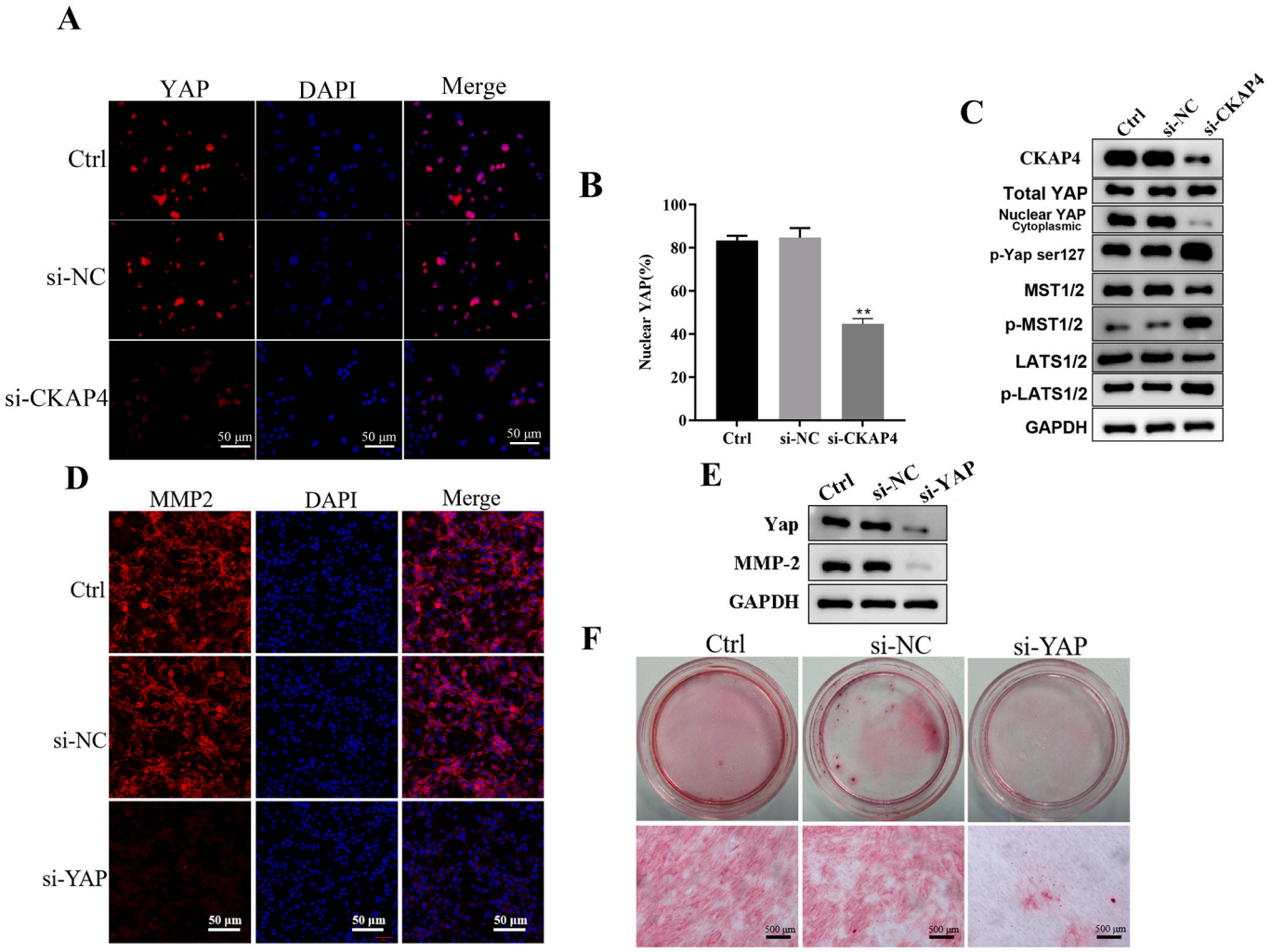

Fig. 3. CKAP4 is associated with nuclear translocation of YAP. (A) Immunofluorescence staining showed nuclear localization of YAP (red) and nuclei (blue) (4, 6-diamidino-2-phenylindole (DAPI)) in VSMCs, cells were treated with negative control, siRNA, or CKAP4 siRNA for 24 h, respectively, Scale bar = 20 μm, $n = 3$. (B) Percentage of cells with predominantly nuclear YAP, n = 3. (C) Western blotting analysis of CKAP4, total YAP, nuclear YAP, phosphorylated YAP S127 (p-YAP s127), MST1/2, p-MST1/2, LATS1 and p-LATS1/2 in whole-cell lysates of VSMCs. Cells were transfected with negative control, siRNA, or CKAP4 siRNA for 24 h, respectively, $n = 3$. (D) Immunofluorescence staining of MMP-2 (red) and DAPI (blue) in VSMCs, cells were treated with negative control siRNA, or YAP siRNA for 24 h, respectively. Scar bars = 20 μm, $n = 3$. (E) Western blotting analysis of YAP and MMP2 of cells treated with control, siRNA, or YAP siRNA, n = 3. (F) Alizarin red staining was performed on VSMCs incubated under different conditions for 14 days with media replacement every 3 days. VSMCs were treated with negative control, siRNA, or YAP siRNA (si-YAP) for 24 h, respectively, $n = 3$. $^{**}P < 0.01$ compared to the si-CTRL group.

through decreased alizarin red staining and aortic calcium levels (Fig. 6A, B). Additionally, western blotting data also indicated that in high Pi-CKD model with si-CKAP4, there was significantly lower YAP and MMP2 levels (Fig. 6C). These results indicated that CKAP4 inhibition attenuates VC through regulation of YAP and MMP2 *in vivo*.

4. Discussion

CKAP4, a transmembrane protein, has been identified to be a cell surface receptor for many proteins such as tissue plasminogen activator (t-PA) and anti-proliferative factor (APF) [34,35]. CKAP4 was shown to inhibit bladder cancer cell proliferation through the attachment of APF [36,37]. Interessantly, t-PA is increased in VSMC and in human atherosclerotic disease, probably as a result of an immunological response to vascular injury. Previously, it was discovered that t-PA binds to CKAP4 and acts as an activator of plasminogen [38]. During our research, we discovered that CKAP4 is substantially elevated in CKD patients (Fig. 1), as well as CKD *in vitro* and *in vivo* models (Fig. 1, 5). Furthermore, we detected enhanced calcification, ALP activity, and apoptosis in these models (Fig. 1, 2, 5). Under a high phosphate environment, cells in the VSMCs model underwent osteogenic differentiation and substantially expressed markers such as Runx2, Msx2, and PIT1, but had lower expression of -SMA and SM22 (Fig. 2F). Previous researchs have shown that Wnt signaling activation promotes osteogenesis in VC [39]. Furthermore, it has been discovered that Wnt signaling induces osteogenic stimulation by activating Runx2 expression [40]. Additionally, in the wnt signaling pathway, prevention of proteasomal degradation of β-catenin, allows its activation and nuclear translocation. This activation of β-catenin, which is a transcriptional regulator of many downstream targets, allow the osteoblast to proliferate and mature [41]. However, the special role of CKAP4 in enhancing osteogenesis, VC and CKD is still unknown.

In the current study, we identified MMP2 to be highly expressed in the serum of CKD patients (Fig. 1B). Interestingly, the silencing of CKAP4 resulted in a decrease in MMP2 expression, as well as calcification and osteogenic differentiation (Fig. 3). Previously, research has clearly revealed that MMP2 may be a significant factor in worsening the severity of CKD [8]. Additionally, it is well established that MMP2 is

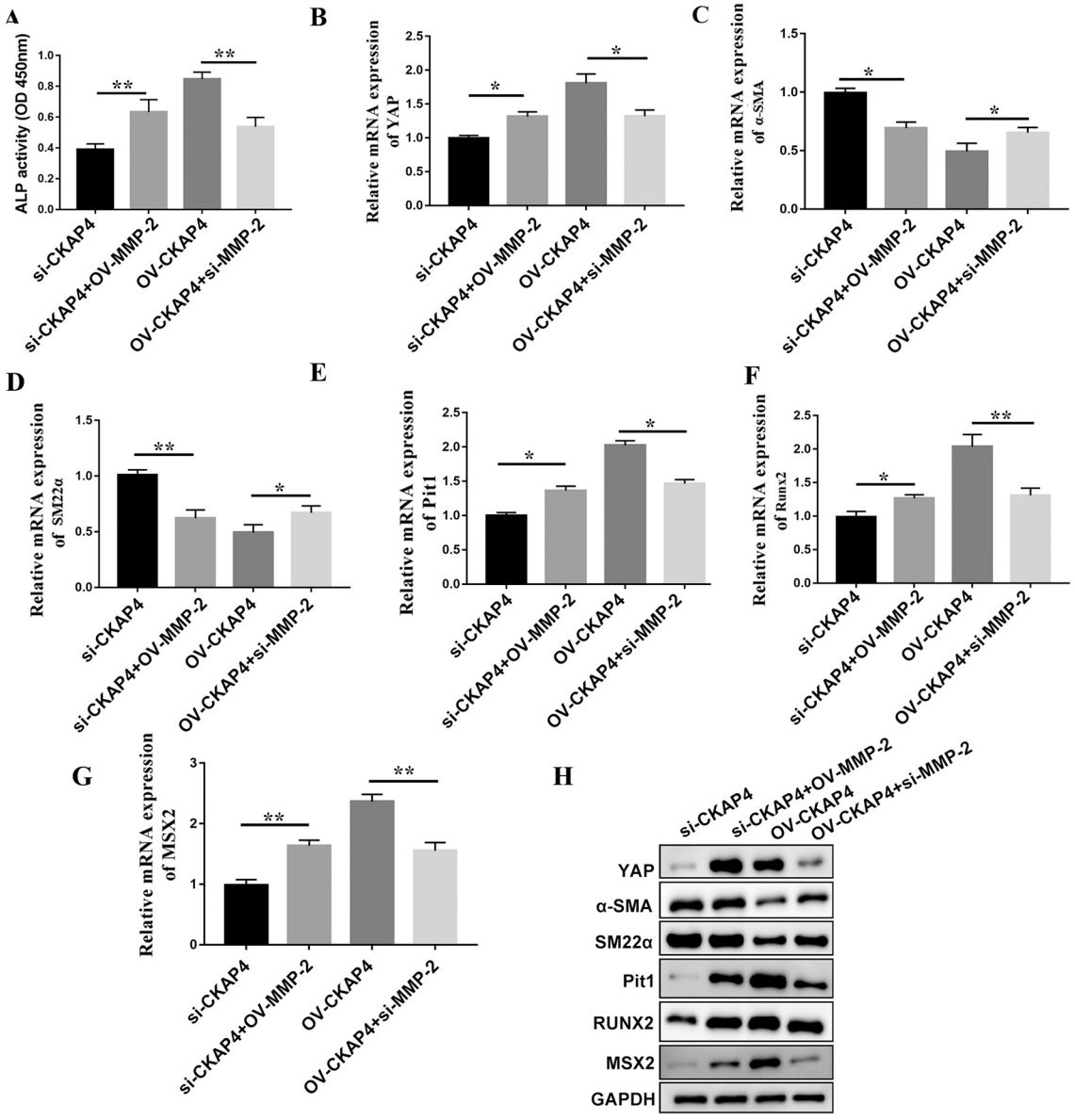

Fig. 4. CKAP4 promotes VSMCs calcification via YAP/MMP-2 pathway. (A) ALP activity was measured by ALP activity assay kit, n = 3. (B-H) Expression of YAP, different smooth cell and osteogenesis marker were determined by qRT-PCR and western blotting in VSMCs exposed to differentiation medium for 24 h. Abbreviations: si-CKAP4, silencing of CKAP4; si-CKAP4 + OV-MMP2, silencing of CKAP4 and overexpression of MMP2; OV-CKAP4, overexpression of CKAP4; OV-CKAP4+ si-MMP2, overexpression of CKAP4 and silencing of MMP2. Values are expressed as mean ± S.E.M ($n = 3$) *$P < 0.05$, **$P < 0.01$.

primarily elevated under oxidative stress and its expression has been known to decrease smooth muscle contraction [42–44]. Chung *et al.*, [45] discovered that increased MMP2 expression is related with reduced glomerular filtration rate and renal function. As a result, it was obvious that MMP2 was related with a worse prognosis in patients with CKD. However, in order to comprehend MMP2's significance in CKD, it is necessary to comprehend how CKAP4 modulates MMP2. To adress this question, we concentrated on YAP, an MMP2 upstream regulator. In our investigation, we discovered that a deficiency of CKAP4 resulted in a decrease in YAP nuclear localization (Fig. 3A, B). Furthermore, the loss of CKAP4 increased phosphorylation of this protein at serine 127, resulting in decreased nucleocytoplasmic localisation (Fig. 3 C). As YAP is an important regulator of many genes, studies have indicated that YAP translocation from nucleus to cytoplasm may result in a reduction in gene transcription of its downstream targets [46]. Other HIPPO pathway factors, such as Mst1/2 and Lats1/2, were likewise markedly reduced in the absence of CKAP4 (Fig. 3C). HIPPO factors in their phosphorylated versions (active HIPPO pathway) are sequestered in the cytoplasm and are found to be transcriptionally inactive. However, inactivation of the HIPPO pathway seems to correspond to nuclear translocation of the factors and activation of YAP [47,48].

YAP antagonists have also been shown in trials to be protective and regenerative in cancer and ischemia [49,50]. In the study by Xu *et al.*, it was clearly indicated that constant increase in YAP activation could cause interstitial fibrosis and abnormal differentiation of renal tubules [50]. According to the findings of our study, nuclear localization and decreased phosphorylation of YAP resulted in increased MMP2 activity, which also contributed in the prevention of VC. YAP has been implicated as an upstream regulator of MMP2 in numerous studies. When YAP was knocked out in stomach cancer trials, MMP2 expression dropped dramatically [51,52]. Even in our study, we observed silencing of YAP significantly decreased MMP2 levels in the *in vitro* model (Fig. 3). We also successfully developed an 5/6 Nx mice model with high phosphate diet, which showed increased calcification, ALP activity and higher

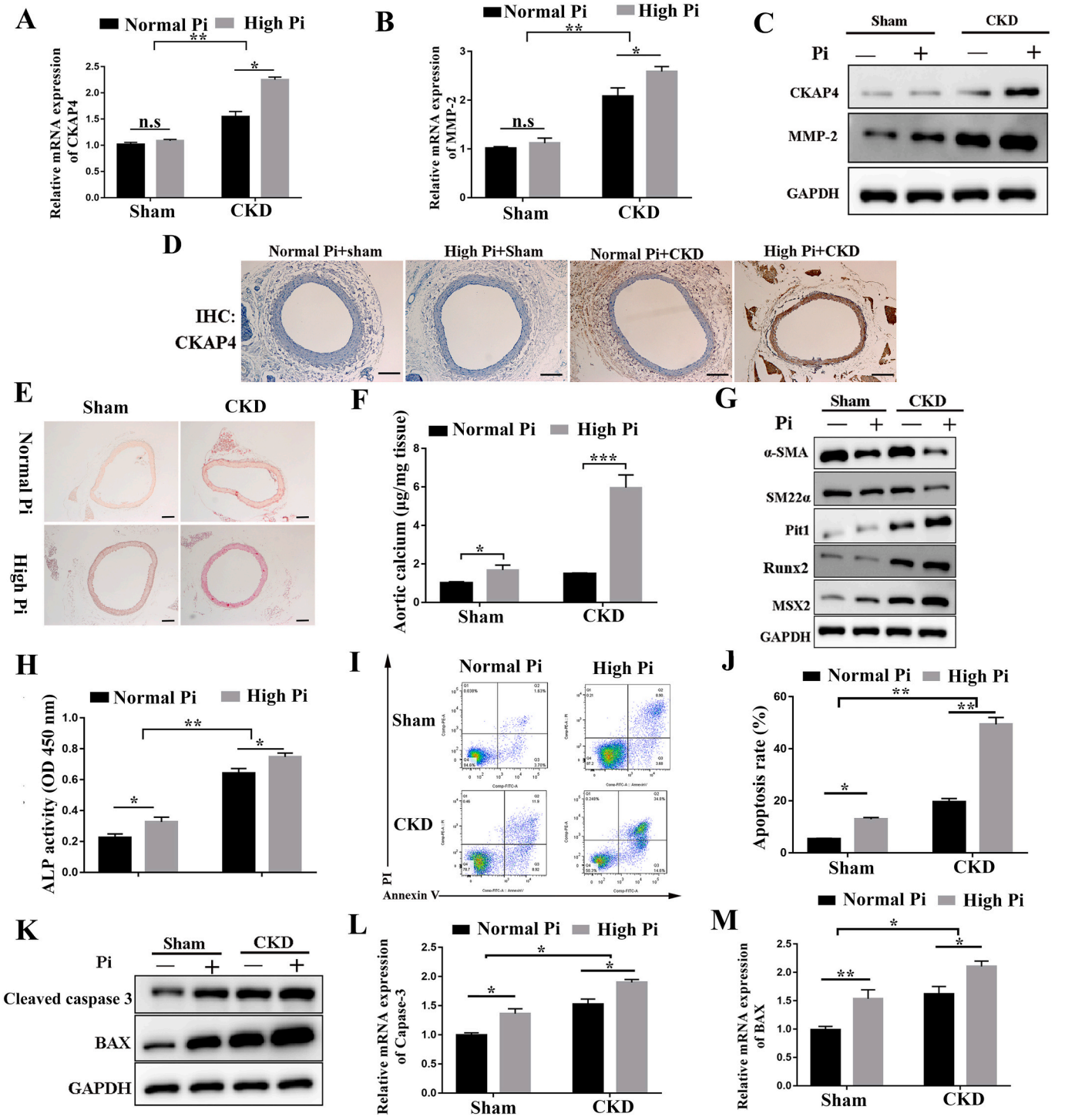

Fig. 5. High Phosphate induces aortic calcification in a high CKD model. (A-C) Expression of CKAP4 and MMP2 were detected by qRT-PCR and western blotting, $n = 6$. (D) Immunohistochemical staining of CKAP4 protein levels, scale bar = 50 μm, n = 6. (E) Representative images of Alizarin Red stained sections of aorta. Scale bar = 50 μm, $n = 6$. (F) Calcium content in the thoracic aorta. n = 6 per group. Data are presented as the mean ± S.E.M. (G) Expression of different smooth cell and osteogenesis marker were detected by western blotting, $n = 6$. (H) ALP activity was measured by ALP activity assay kit, n = 6. (I,J) Analysis of apoptosis rates by flow cytometry and quantification, n = 6. (K-M) mRNA expression of *Capase-3* and *Bax* detected by qRT-PCR and western blotting, n = 6. Data are expressed as the mean ± S.E.M. $^{*}P < 0.05$, $^{**}P < 0.01$, $^{***}P < 0.001$.

osteogenic expression profile (Fig. 5). However, silencing of CKAP4 in the CKD mice model, showed significant decrease YAP, MMP2 and calcification (Fig. 6). This confirmed our hypothesis, CKAP4 modulates YAP phosphorylation and MMP2 expression, which contributes to VC development in patients with CKD.

Funding

The National Natural Science Foundation of China (No. 81970636).

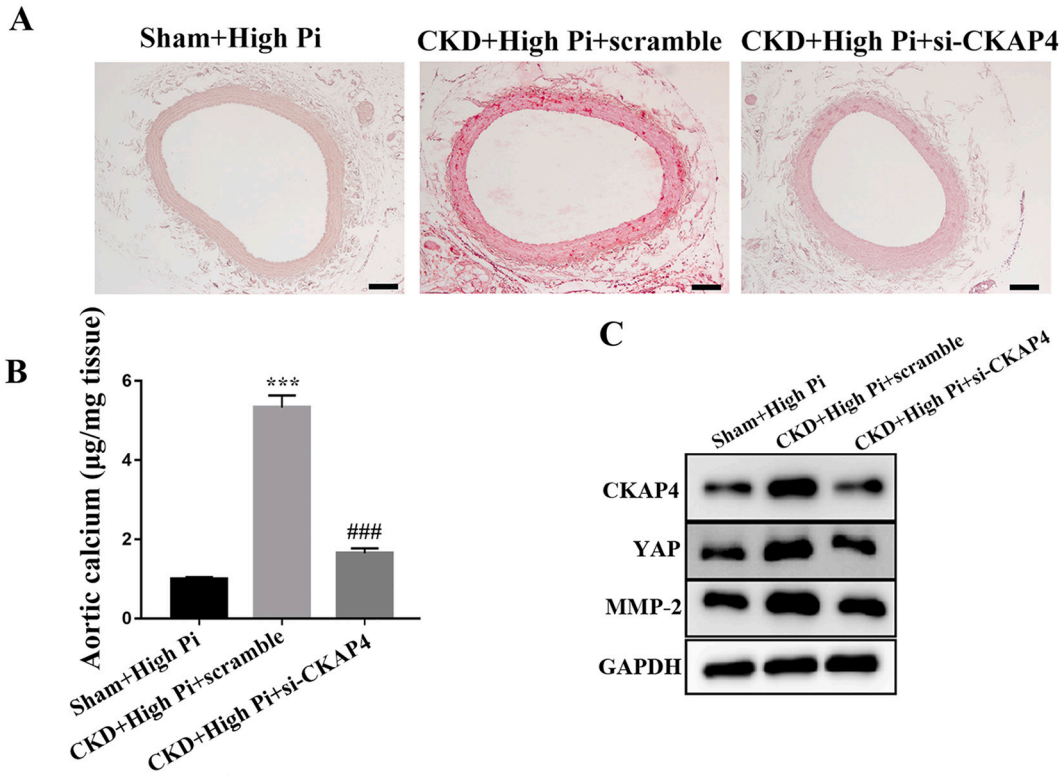

Fig. 6. CKAP4 inhibition attenuates vascular calcification in CKD mice. CKD mice were administered with scramble or si-CKAP4 lentivirus via tail vein injection and placed on high phosphate diet for 12 weeks. (A) Representative images of alizarin red stained sections of aorta. Scale bar = 50 μm, $n = 6$. (B) Calcium content in the tissues of thoracic aorta. n = 6 per group. Data are presented as the mean ± S.E.M. $^{*}P < 0.05$, $^{***}P < 0.001$ vs. Sham + High Pi, ###P < 0.001 vs CKD + High Pi + scramble. (C) Expression of CKAP4, YAP, MMP2 were detected by western blotting, n = 6.

Declaration of Competing Interest

No potential conflicts of interest are disclosed.

Acknowledgements

None.

References

[1] N.R. Hill, F.S. T, O.J. L, H.J. A, O.C.C. A, L.D. S, H.F.D. Richard, R. Giuseppe, Global prevalence of chronic kidney disease – a systematic review and meta-analysis, PLoS One 11(7) e0158765.
[2] K. Brück, V.S. Stel, G. Gambaro, S. Hallan, H. Völzke, J. Ärnlöv, M. Kastarinen, I. Guessous, J. Vinhas, B. Stengel, H. Brenner, J. Chudek, S. Romundstad, C. Tomson, A.O. Gonzalez, A.K. Bello, J. Ferrieres, L. Palmieri, G. Browne, V. Capuano, W. Van Biesen, C. Zoccali, R. Gansevoort, G. Navis, D. Rothenbacher, P.M. Ferraro, D. Nitsch, C. Wanner, K.J. Jager, CKD prevalence varies across the european general population, J. Am. Soc. Nephrol. 27 (7) (2016) 2135–2147.
[3] J.R. Paniagua-Sierra, M.E. Galván-Plata, Chronic kidney disease, Rev. Med. Inst. Mex. Seguro. Soc. 55 (Suppl. 2) (2017) S116–S117.
[4] Y. Chen, X. Zhao, H. Wu, Arterial stiffness: a focus on vascular calcification and its link to bone mineralization, Arterioscler. Thromb. Vasc. Biol. 40 (5) (2020).
[5] L. Feng, D. Que, Z. Li, X. Zhong, J. Yan, J. Wei, X. Zhang, P. Yang, C. Ou, M. Chen, Dihydromyricetin ameliorates vascular calcification in chronic kidney disease by targeting AKT signaling, Clin. Sci. (London, England : 1979) 135 (21) (2021) 2483–2502.
[6] L.A. Pescatore, L.F. Gamarra, M. Liberman, Multifaceted mechanisms of vascular calcification in aging, Arterioscler. Thromb. Vasc. Biol. 39 (7) (2019) 1307–1316.
[7] R. Neto, L. Pereira, J. Magalhães, J. Quelhas-Santos, J. Frazão, Low bone turnover is associated with plain X-ray vascular calcification in predialysis patients, PLoS One 16 (10) (2021), e0258284.
[8] A.W.Y. Chung, H.H.C. Yang, J.M. Kim, M.K. Sigrist, E. Chum, W.A. Gourlay, A. Levin, Upregulation of matrix metalloproteinase-2 in the arterial vasculature contributes to stiffening and vasomotor dysfunction in patients with chronic kidney disease, Circulation 120 (9) (2009) 792–801.
[9] K.R. Tuttle, G.L. Bakris, R.W. Bilous, J.L. Chiang, I.H. de Boer, J. Goldstein-Fuchs, I. B. Hirsch, K. Kalantar-Zadeh, A.S. Narva, S.D. Navaneethan, J.J. Neumiller, U. D. Patel, R.E. Ratner, A.T. Whaley-Connell, M.E. Molitch, Diabetic kidney disease: a report from an ADA Consensus Conference, Am. J. Kidney Dis. 64 (4) (2014) 510–533.
[10] V. Papademetriou, L. Lovato, M. Doumas, E. Nylen, A. Mottl, R.M. Cohen, W. B. Applegate, Z. Puntakee, J.F. Yale, W.C. Cushman, Chronic kidney disease and intensive glycemic control increase cardiovascular risk in patients with type 2 diabetes, Kidney Int. 87 (3) (2015) 649–659.
[11] M. Wu, C. Rementer, C.M. Giachelli, Vascular calcification: an update on mechanisms and challenges in treatment, Calcif Tissue Int. 93 (4) (2013) 365–373.
[12] R.D. Kenagy, S. Vergel, E. Mattsson, M. Bendeck, M.A. Reidy, A.W. Clowes, The Role of Plasminogen, Plasminogen Activators, and Matrix Metalloproteinases in Primate Arterial Smooth Muscle Cell Migration 16(11), 1996, p. 1373.
[13] J.M. Munro, R.S. Cotran, The Pathogenesis of Atherosclerosis: Atherogenesis and Inflammation 58(3), 1989, pp. 249–261.
[14] S. Mathew, K.S. Tustison, T. Sugatani, L.R. Chaudhary, L. Rifas, K.A. Hruska, The Mechanism of Phosphorus as a Cardiovascular Risk Factor in CKD 19(6), 2008, pp. 1092–1105.
[15] Reynolds, J. L., Human vascular smooth muscle cells undergo vesicle-mediated calcification in response to changes in extracellular calcium and phosphate concentrations: a potential mechanism for accelerated vascular calcification in ESRD, J. Am. Soc. Nephrol. 15(11) 2857-2867.
[16] J.B. Cannata-Andia, P. Roman-Garcia, K. Hruska, The connections between vascular calcification and bone health, Nephrol. Dial. Transplant. 26 (11) (2011) 3429–3436.
[17] R.C. Shroff, R. McNair, J.N. Skepper, N. Figg, L.J. Schurgers, J. Deanfield, L. Rees, C.M. Shanahan, Chronic mineral dysregulation promotes vascular smooth muscle cell adaptation and extracellular matrix calcification, J. Am. Soc. Nephrol. 21 (1) (2010) 103–112.
[18] J.J. Patel, L.E. Bourne, B.K. Davies, T.R. Arnett, V.E. MacRae, C.P. Wheeler-Jones, I.R. Orriss, Differing calcification processes in cultured vascular smooth muscle cells and osteoblasts, Exp. Cell Res. 380 (1) (2019) 100–113.
[19] D. Ge, N. Meng, L. Su, Y. Zhang, S.-l. Zhang, J.-y. Miao, J. Zhao, Human vascular endothelial cells reduce sphingosylphosphorylcholine-induced smooth muscle cell contraction in co-culture system through integrin β4 and Fyn, Acta Pharmacol. Sin. 33 (1) (2012) 57–65.
[20] Kimura, Hirokazu, Fumoto, Katsumi, Shojima, Kensaku, Nojima, Satoshi, Osugi, Yoshihito, CKAP4 is a Dickkopf1 receptor and is involved in tumor progression, J. Clin. Investig.
[21] H. Kimura, H. Yamamoto, T. Harada, K. Fumoto, Y. Osugi, R. Sada, N. Maehara, H. Hikita, S. Mori, H. Eguchi, M. Ikawa, T. Takehara, A. Kikuchi, CKAP4, a DKK1 receptor, is a biomarker in exosomes derived from pancreatic cancer and a molecular target for therapy, Clin. Cancer Res. 25 (6) (2019) 1936–1947.

[22] S. Thambiah, R. Roplekar, P. Manghat, I. Fogelman, W.D. Fraser, D. Goldsmith, G. Hampson, Circulating sclerostin and Dickkopf-1 (DKK1) in predialysis chronic kidney disease (CKD): relationship with bone density and arterial stiffness, Calcif. Tissue Int. 90 (6) (2012) 473–480.
[23] H. Shahjee, K. Koch, L. Guo, C. Zhang, S. Keay, Antiproliferative factor decreases Akt phosphorylation and alters gene expression via CKAP4 in T24 bladder carcinoma cells, J. Exp. Clin. Cancer Res. 29 (2010) 160.
[24] A. Chung, H. Yang, J.M. Kim, M.K. Sigrist, E. Chum, W.A. Gourlay, A. Levin, Upregulation of matrix metalloproteinase-2 in the arterial vasculature contributes to stiffening and vasomotor dysfunction in patients with chronic kidney disease, Circulation 120 (9) (2009) 792–801.
[25] T. Zheng, X. Liu, X. Li, Q. Wang, Y. Zhao, X. Li, M. Li, Y. Zhang, M. Zhang, W. Zhang, C. Zhang, Y. Zhang, M. Zhang, Dickkopf-1 promotes Vascular Smooth Muscle Cell proliferation and migration through upregulating UHRF1 during Cyclic Stretch application, Int. J. Biol. Sci. 17 (5) (2021) 1234–1249.
[26] J. Zhang, Z.P. Xu, Y.C. Yang, J.S. Zhu, W.X. Chen, Expression of Yes-associated protein in gastric adenocarcinoma and inhibitory effects of its knockdown on gastric cancer cell proliferation and metastasis, Int. J. Immunopathol. Pharmacol. 25 (3) (2012) 583.
[27] X. Jin, R. Shu, W. Yuan, L. Gu, J. Jia, W. Ling, H. Yu, Z. Yifeng, High mobility group box 1 promotes aortic calcification in chronic kidney disease via the Wnt/β-catenin pathway, Front. Physiol. 9 (2018) 665.
[28] I. Kanazawa, T. Yamaguchi, S. Yano, M. Yamauchi, M. Yamamoto, T. Sugimoto, Adiponectin and AMP kinase activator stimulate proliferation, differentiation, and mineralization of osteoblastic MC3T3-E1 cells, BMC Cell Biol. 8 (2007).
[29] X. Lin, J.-K. Zhan, J.-Y. Zhong, Y.-J. Wang, Y. Wang, S. Li, J.-Y. He, P. Tan, Y.-Y. Chen, X.-B. Liu, X.-J. Cui, Y.-S. Liu, lncRNA-ES3/miR-34c-5p/BMF axis is involved in regulating high-glucose-induced calcification/senescence of VSMCs, Aging 11 (2) (2019) 523–535.
[30] C. Li, Y. Chang, Y. Li, S. Chen, Y. Chen, N. Ye, D. Dai, Y. Sun, Advanced glycation end products promote the proliferation and migration of primary rat vascular smooth muscle cells via the upregulation of BAG3, Int. J. Mol. Med.
[31] N. Wu, X. Lin, X. Zhao, L. Zheng, L. Xiao, J. Liu, L. Ge, S. Cao, MiR-125b acts as an oncogene in glioblastoma cells and inhibits cell apoptosis through p53 and p38MAPK-independent pathways, Br. J. Cancer 109(11) 2853-2863.
[32] S. Rong, X. Zhao, X. Jin, Z. Zhang, W. Yuan, Vascular Calcification in Chronic Kidney Disease is Induced by Bone Morphogenetic Protein-2 via a Mechanism Involving the Wnt/β-Catenin Pathway, Cell. Physiol. Biochem. Int. 34 (6) (2014) 2049–2060.
[33] Taha, Azad, Mina, Ghahremani, Xiaolong, Yang, The Role of YAP and TAZ in Angiogenesis and Vascular Mimicry.
[34] T.P. Conrads, G.M. Tocci, B.L. Hood, C.-O. Zhang, L. Guo, K.R. Koch, C.J. Michejda, T.D. Veenstra, S.K. Keay, CKAP4/p63 is a receptor for the frizzled-8 protein-related antiproliferative factor from interstitial cystitis patients, J. Biol. Chem. 281(49) 37836-37843.
[35] S.R. Bates, A.S. Kazi, J.-Q. Tao, K.J. Yu, D.S. Gonder, S.I. Feinstein, A.B. Fisher, Role of P63 (CKAP4) in binding of surfactant protein-A to type II pneumocytes, Lung Cell. Mol. Physiol.: 295(4) L658-L669.
[36] S.X. Li, L.-j. Liu, L.-w. Dong, H.-g. Shi, Y.-f. Pan, Y.-x. Tan, J. Zhang, B. Zhang, Z.-w. Ding, T.-y. Jiang, CKAP4 inhibited growth and metastasis of hepatocellular carcinoma through regulating EGFR signaling, Tumour Biol. 35(8) 7999-8005.
[37] H.M. Shahjee, K.R. Koch, L. Guo, Antiproliferative Factor Decreases Akt Phosphorylation and Alters Gene Expression Via CKAP4 in T24 Bladder Carcinoma Cells, 29(1) 160.
[38] T.M. Razzaq, R. Bass, D.J. Vines, F. Werner, S.A. Whawell, V. Ellis, Functional regulation of tissue plasminogen activator on the surface of vascular smooth muscle cells by the type-II transmembrane protein p63 (CKAP4), J. Biol. Chem. 278 (43) 42679-42685.
[39] J.M. Martínez-Moreno, J.R. Muñoz-Castañeda, C. Herencia, A.M.D. Oca, J. C. Estepa, R. Canalejo, M.E. Rodríguez-Ortiz, P. Perez-Martinez, E. Aguilera-Tejero, A. Canalejo, In Vascular Smooth Muscle Cells Paricalcitol Prevents Phosphate-induced Wnt/β-catenin Activation 303(8), 2012, p. F1136.
[40] T. Gaur, C.J. Lengner, H. Hovhannisyan, R.A. Bhat, J.B. Lian, Canonical WNT signaling promotes osteogenesis by directly stimulating Runx2 gene expression, J. Biol. Chem. 280 (39) (2005) 33132–33140.
[41] R. Nusse, H. Clevers, Wnt/β-catenin signaling, disease, and emerging therapeutic modalities, Cell 169 (6) (2017) 985–999.
[42] W. Wang, S. Viappiani, J. Sawicka, R. Schulz, Inhibition of endogenous nitric oxide in the heart enhances matrix metalloproteinase-2 release, Br. J. Pharmacol. 145 (1) (2005) 43–49.
[43] D.K.W. Chew, M.S. Conte, R.A. Khalil, Matrix metalloproteinase-specific inhibition of Ca2+ entry mechanisms of vascular contraction, J. Vasc. Surg. 40 (5) (2004) 1001–1010.
[44] Z.S. Galis, J.J. Khatri, Matrix metalloproteinases in vascular remodeling and atherogenesis: the good, the bad, and the ugly, Circ. Res. 90 (3) (2002) 251–262.
[45] A.W. Chung, A.D. Booth, C. Rose, C.R. Thompson, A. Levin, C. van Breemen, Increased matrix metalloproteinase 2 activity in the human internal mammary artery is associated with ageing, hypertension, diabetes and kidney dysfunction, J. Vasc. Res. 45(4) 357-362.
[46] M. Sudol, D.C. Shields, A. Farooq, Structures of YAP protein domains reveal promising targets for development of new cancer drugs, Semin. Cell Dev. Biol. 23 (7) 827-833.
[47] B. Zhao, X. Wei, W. Li, R.S. Udan, Q. Yang, J. Kim, J. Xie, T. Ikenoue, J. Yu, L. Li, Inactivation of YAP oncoprotein by the Hippo pathway is involved in cell contact inhibition and tissue growth control, Genes Dev. 21(21) 2747-2761.
[48] B. Zhao, K. Tumaneng, K.-L. Guan, The Hippo pathway in organ size control, tissue regeneration and stem cell self-renewal, Nat. Cell Biol. 13(8) 877-883.
[49] S. Jiao, H. Wang, Z. Shi, A. Dong, Z. Zhou, A peptide mimicking VGLL4 function acts as a YAP antagonist therapy against gastric cancer, Cancer Cell 25 (2) (2014) 166–180.
[50] J. Xu, P.-X. Li, J. Wu, Y.-J. Gao, M.-X. Yin, Y. Lin, M. Yang, D.-P. Chen, H.-P. Sun, Z.-B. Liu, Involvement of the Hippo pathway in regeneration and fibrogenesis after ischaemic acute kidney injury: YAP is the key effector, Clin. Sci. 130 (2016) 349–363.
[51] J. Zhang, Z.P. Xu, Y.C. Yang, J.S. Zhu, Z. Zhou, W.X. Chen, Expression of Yes-associated Protein in Gastric Adenocarcinoma and Inhibitory Effects of its Knockdown on Gastric Cancer Cell Proliferation and Metastasis 25(3), 2012, p. 583.
[52] Z. Pan, Y. Tian, B. Zhang, X. Zhang, H. Shi, Z. Liang, P. Wu, R. Li, B. You, L. Yang, YAP signaling in gastric cancer-derived mesenchymal stem cells is critical for its promoting role in cancer progression, Int. J. Oncol.